Supporting Information

Two fluorescent signal indicators-based ratio fluorometric alkaline phosphatase assay based on one signal precursor

Rongji Wang,[a] Zhihua Wang,*[a] Honghong Rao,[b] Xin Xue,[a] Mingyue Luo,[a] Zhonghua Xue*[a] and Xiaoquan Lu[a]

[a]*Key Laboratory of Bioelectrochemistry & Environmental Analysis of Gansu Province, College of Chemistry & Chemical Engineering, Northwest Normal University, Lanzhou, 730070 (China)*

[b]*School of chemistry & Chemical Engineering, Lanzhou City University, Lanzhou, 730070, China.*
E-mail address: xzh@nwnu.edu.cn (Z. H. Xue); wangzh@nwnu.edu.cn (Z. H. Wang).

Experimental Section

Chemicals and Materials. O-phenylenediamine (OPD), hydrochloric acid (HCl), sodium vanadate (Na_3VO_4), L-ascorbic acid 2-phosphate trisodium salt (AAP) and tetramethy-lammonium hydroxide (TMA·OH) were purchased from Aladdin Industrial Corporation (Shanghai, China). phenylenediamine (MPD) and p-phenylenediamine (PPD) were obtained from Beijing Chemical Reagent Corporation (China). Tris-(hydroxymethyl)-aminomethane (Tris) was purchased from Sigma-Aldrich. $MnCl_2·4H_2O$ and H_2O_2 (30%) were obtained from Beijing Chemical Corporation (Beijing, China). Ascorbic acid (AA) was obtained from Shanghai Zhongqin Chemical Reagent Co. Ltd. (Shanghai, China). The interfering substances including horseradish peroxidase (HRP), alkaline phosphatase (ALP), Cellulase, Protease, acetylcholine-esterase (AChE), Trypsin (Try), Lysozyme (Lys), glucose oxidase (GOx), and bovine serum albumin (BSA) were purchased from Sigma-Aldrich. Unless otherwise stated, chemicals in all the experiments were analytical reagent grade. Human serum specimens were derived from Hospital 940 of PLA Joint Logistics Support Force (Gansu, China). All aqueous solutions were prepared by using deionized water (>18.25 MΩ cm).

Instrumentes. Fluorescence spectra and ultraviolet-visible (UV-vis) spectra measurements were carried out with a FluoroMax-4 spectrofluorometer (Tokyo) and an Agilent 8453 UV-vis spectrophotometer (Agilent Inc., Jpn), respectively. Constant warm water bath (Jing Hong DK-S24, China) was employed for incubating enzyme. TEM images were acquired by using FEI electron microscopy (TECNAI, G2 F20 S-TWIN, US) with an Energy dispersive X-ray spectroscopy (EDS) (Gatan 832, EDX) operating at an accelerating voltage of 5 kV. FT-IR spectra was obtained using a Broker Optics FTS3000 spectrometer (DIGI-LAB, USA) in the transmission mode. The X-ray photoelectron spectroscopy (XPS) was recorded by using Thermo Fisher Scientific (ESCALAB 250Xi, USA). The real pH value of different buffer solutions were measured by a Metrohm 632 pH-meter. Centrifugation was performed on a Ke Cheng H3-18K centrifuge.

Preparation of MnO_2 Nanosheets. MnO_2 nanosheets were prepared according to the literature with minor modifications. Typically, 10 mL of $MnCl_2·4H_2O$ (0.3 M) and 20 mL of TMA·OH (0.6 M) containing 30 wt % of H_2O_2 were immediately mixed in a 100 mL round-bottomed flask. The obtained dark brown solution was stirred vigorously in the open air at room temperature for 12 h. After that, MnO_2 nanosheets were obtained after centrifugation at 10000 rpm for 15 min, and then washed five times with ultrapure water and methanol, respectively. Finally, the precipitate was dried at 50 °C. Prior to study the sensing performance of MnO_2 nanosheets system, the as-

prepared MnO_2 nanosheets were dispersed into ultrapure water by ultrasonication to form a brown colloid.

Sensing ALP Activity. For ratio fluorometric sensing ALP activity, 20 μL of ALP with different concentrations (final concentration 0, 0.25, 0.5, 1, 1.5, 3, 5, 7, 10, 20, 40, 60, 80, 100, 150, and 200 mU/mL) was respectively added into 1790 μL of Tris-HCl buffer (pH 7.4, 20 mM) containing 10 μL of MnO_2 nanosheets dispersion (1 mg/mL), 100 μL of AAP (10 mM) and 80 μL of deoxygenated OPD (20 mM). After reacting in the dark at 37 °C for ~50 min, the fluorescence spectra of different systems was recorded from 430 nm to 563 nm upon an excitation light source with 375 nm wavelength.

Specificity of the Sensing System. To further investigate the specificity of this proposed sensing system toward ALP activity, the fluorescence intensity responses (F_{563}/F_{430}) of the sensing system were recorded for the reaction solution in the absence and presence of ALP (8 mU/mL) with the introduction of the different interferences substances such as HRP, Trypsin, AChE, Lysozyme, Cellulase, Gox, BSA and Protease with a higher concentration (80 mU/mL).

Sensing ALP Activity in Human Serum Samples. To assess the real application feasibility of this developed ratio fluorometric bioassay, ALP levels in human serum was tested by using the standard addition method. Specifically, 100 μL of the diluted human serum solutions with different spiked standard ALP samples (0, 1, and 4 mU/mL) were respectively added into the reaction solution (1710 μL Tris-HCl buffer solutions) that containing 10 μL of MnO_2 nanosheets (1 mg/mL), 100 μL of AAP (10 mM) and 80 μL of deoxygenated OPD and keeping incubation at 37 °C for 50 min. After that, the samples were suffered to the fluorescent analysis according to the described method above. (Here we state that all experiments were performed in accordance with the Guidelines on Administration of Lab, and approved by the ethics committee at Northwest Normal University. Study participants were fully informed regarding the purposes of the study and consent was obtained.)

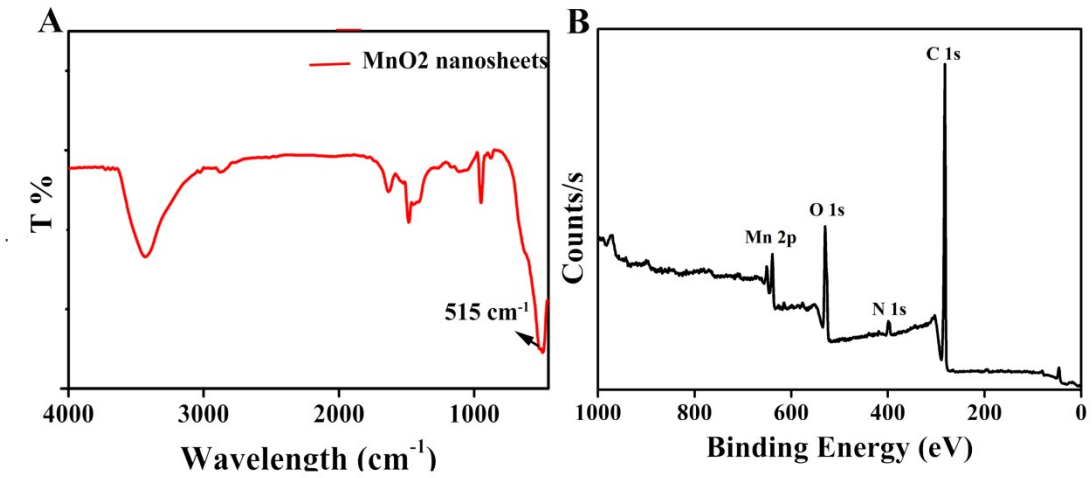

Fig. S1. Characterization of MnO_2 nanaosheets (A) FT-IR spectra (B) A wide scan XPS spectrum.

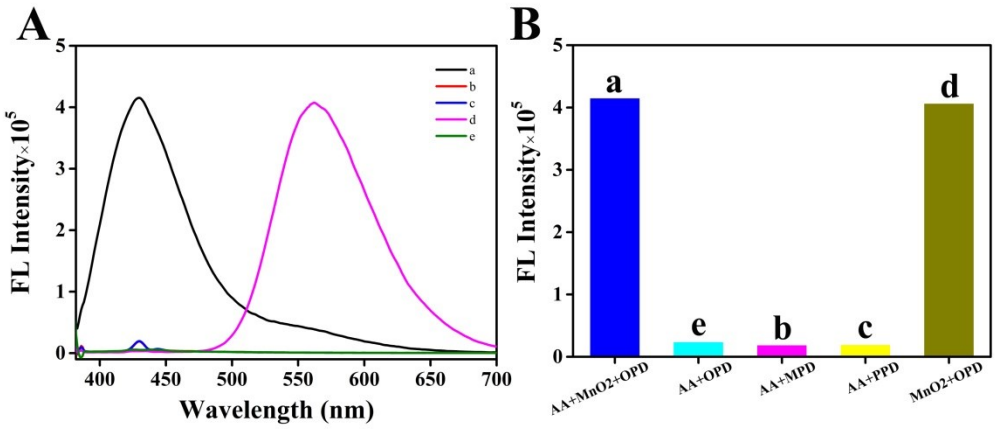

Fig. S2 Fluorescence spectra (A) and fluorescence intensities (B) of the reaction system of AA in the presence of MnO_2 and OPD (a); MPD (b); PPD (c); OPD+MnO_2 (d); AA+OPD (e). The final concentration of AA (1 mM); PPD, MPD and OPD (1 mM); MnO_2 (5 μg/mL). λex=375 nm; incubation time (50 min).

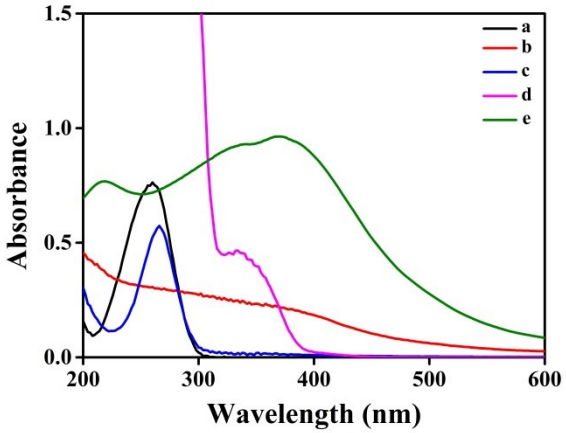

Fig. S3. UV-vis spectra of different reaction system in the Tris-HCl buffer solution (a) 0.1 mM of AA; (b) 0.05 mM AA and 5 μg/mL MnO_2; (c) 0.1 mM AA and 5 μg/mL MnO_2; (d) 0.1 mM AA and 5 μg/mL MnO_2 and 0.8 mM OPD; (e) 5 μg/mL MnO_2.

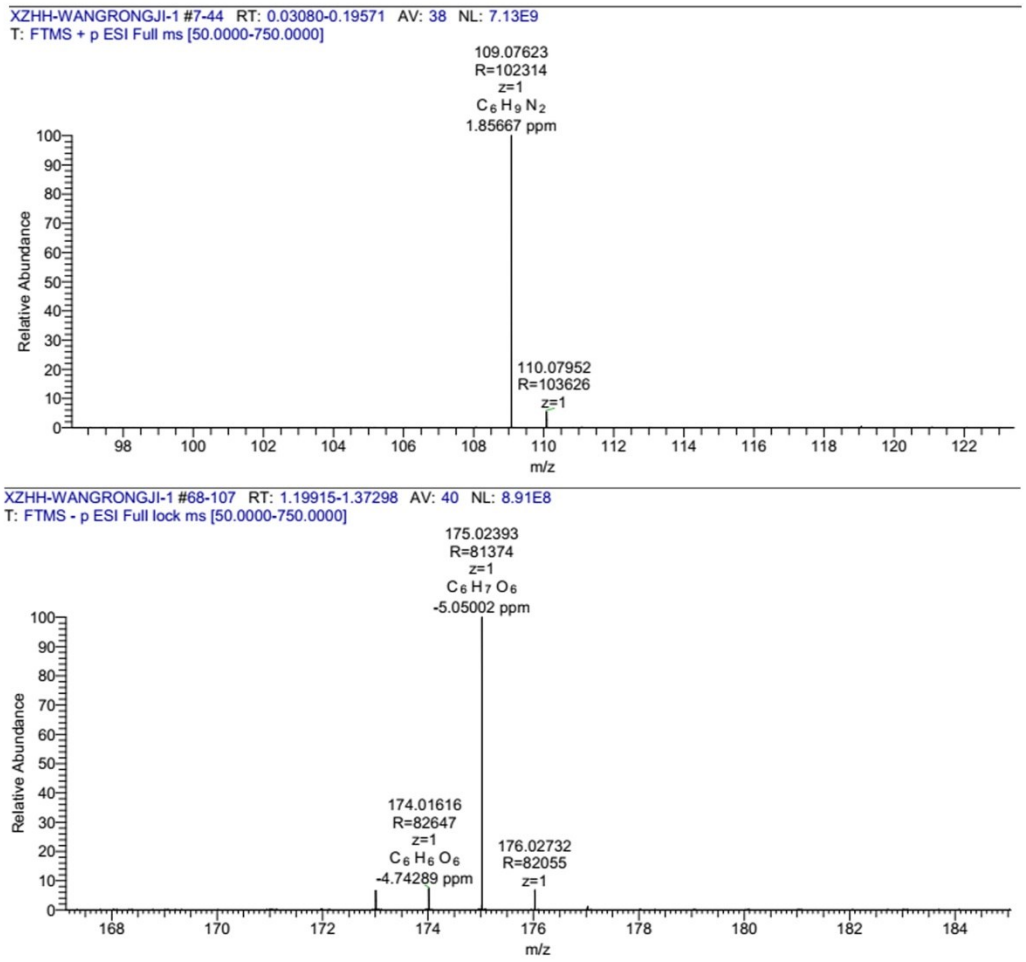

Fig. S4. The mass spectrum of the reaction system of AA and OPD in the absence of MnO_2 nanosheets in the system.

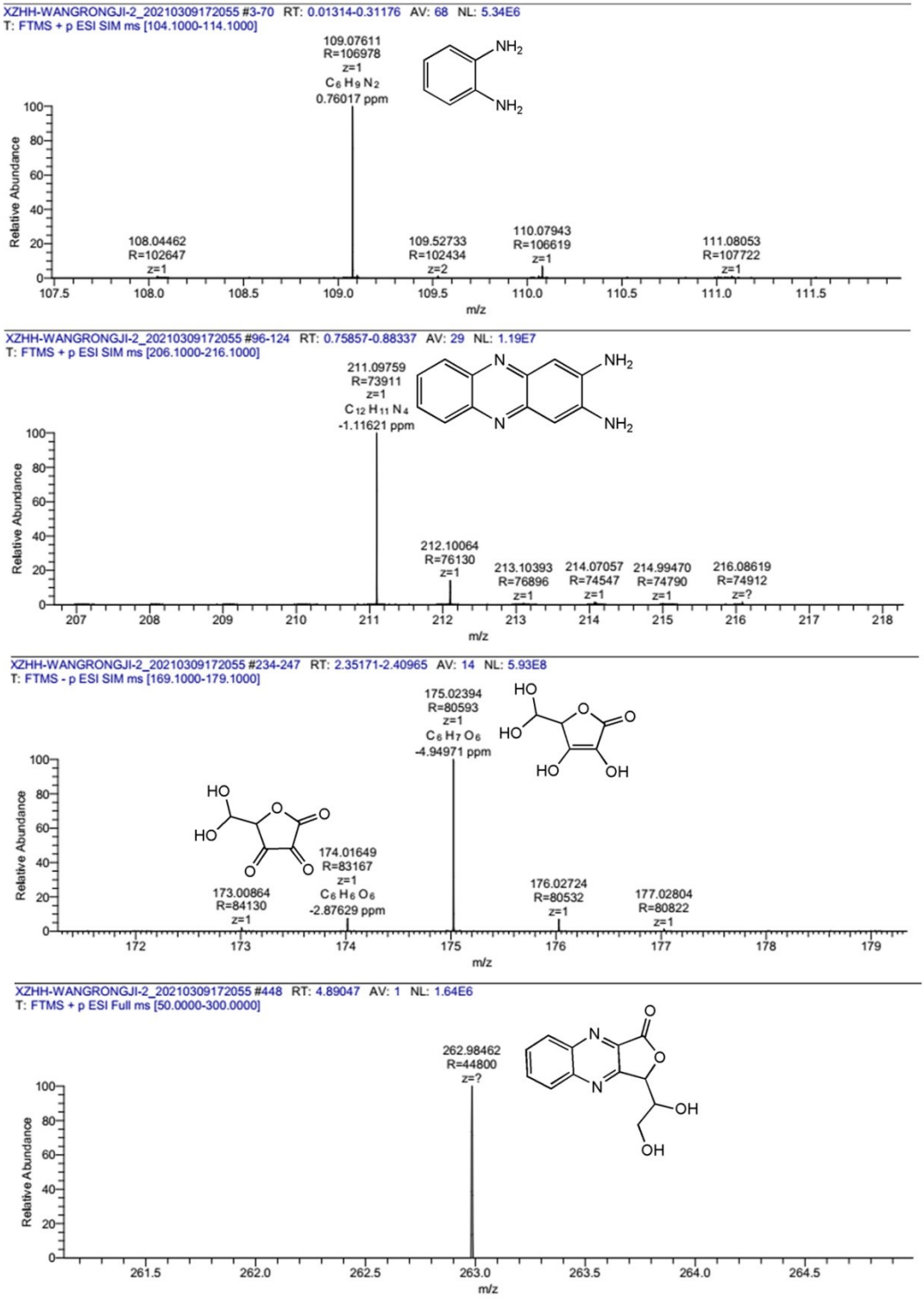

Fig.S5. The mass spectrum of the reaction system of AA and OPD in the presence of MnO_2 nanosheets. DFQ was obtained with anions mode $[M+OH]^-$.

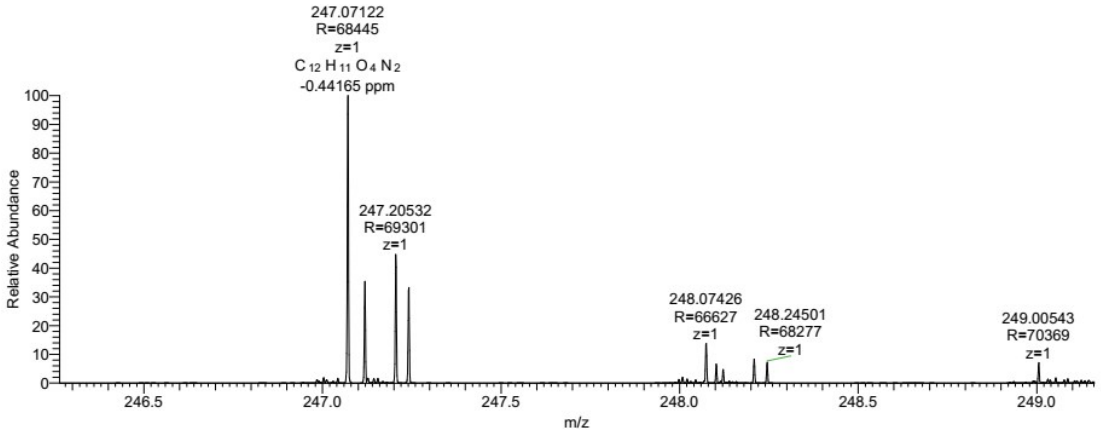

Fig. S6. The mass spectrum of the reaction system containing MnO_2, OPD, ALP and AAP. DFQ was obtained with cationic mode $[M+H]^+$.

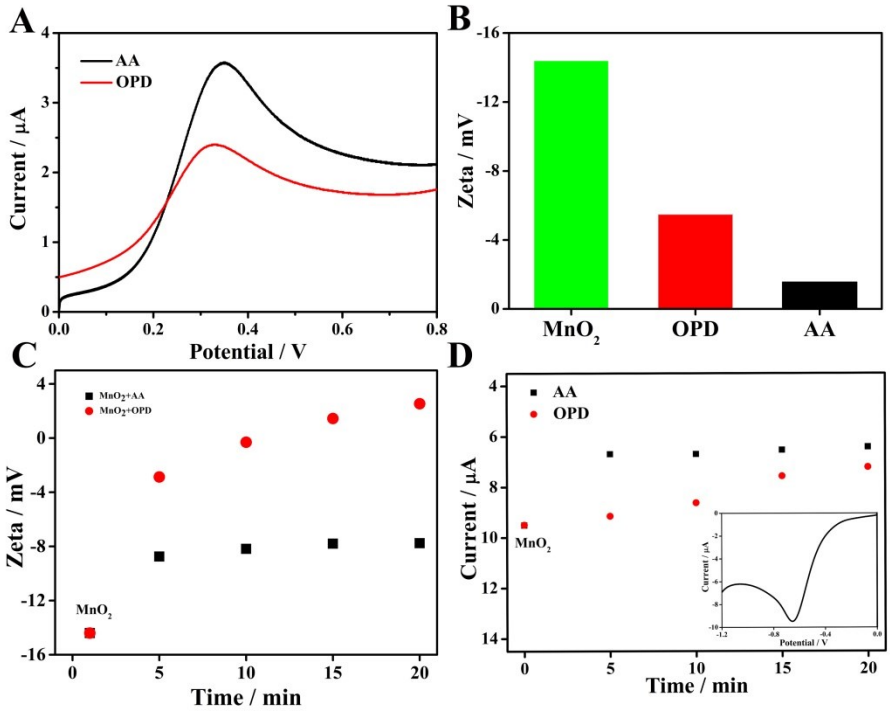

Fig. S7. (A) Linear sweep voltammetry of AA and OPD at bare glass carbon electrode. (B) Zeta potential of MnO_2 nanosheets, OPD and AA. (C) Zeta potentials-time plot and of the reaction system of MnO_2 nanosheets with the addition of AA and OPD, respectively. (D) Reduction currents-time plot of MnO_2 nanosheets at bare glass carbon electrode (at -0.654 V) with the addition of AA and OPD. Insert: Linear sweep voltammetry of MnO_2 nanosheets at bare glass carbon electrode.

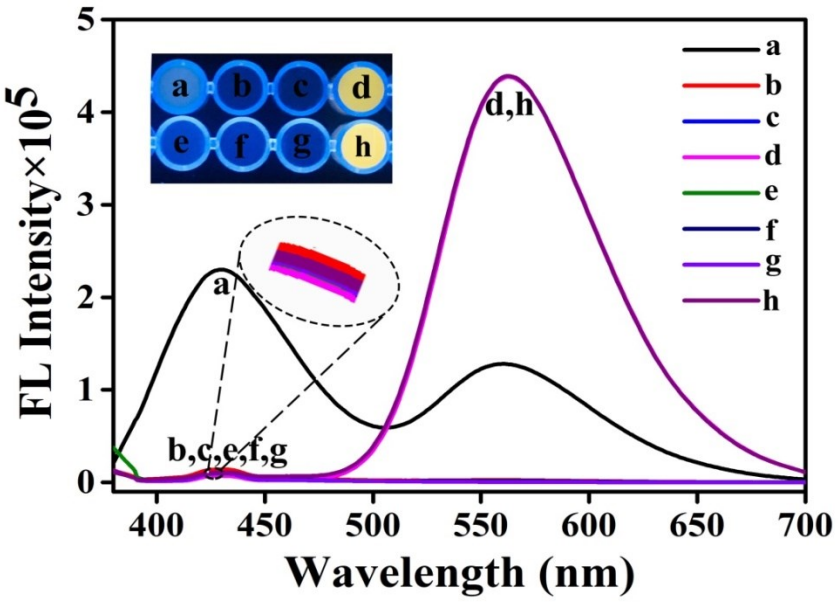

Fig. S8. Fluorescence emission spectra of (a) AAP+ ALP+MnO_2+OPD; (b) AAP+MnO_2+ALP; (c) AAP+MnO_2; (d) ALP+MnO_2+OPD; (e) AAP+OPD; (f) ALP+OPD; (g) AAP+ALP+OPD; h: MnO_2+AAP+OPD.in the Tris-HCl pH 7.4 buffer solution.

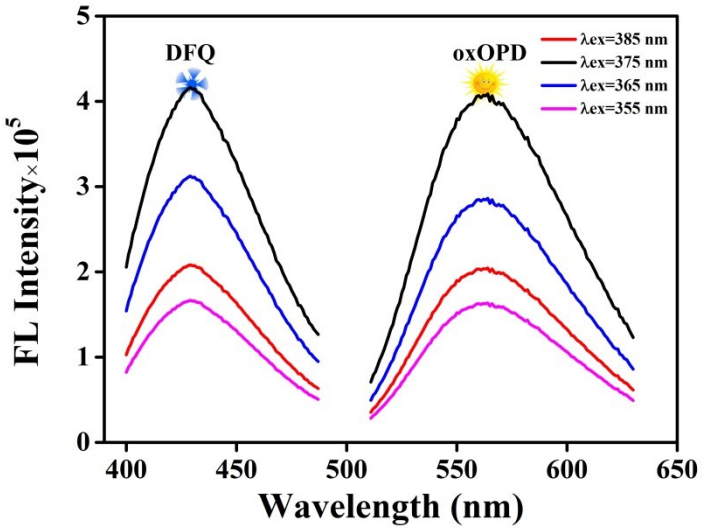

Fig. S9. Fluorescence peaks of DFQ and oxOPD in the proposed system at various excitation light source with different wavelength.

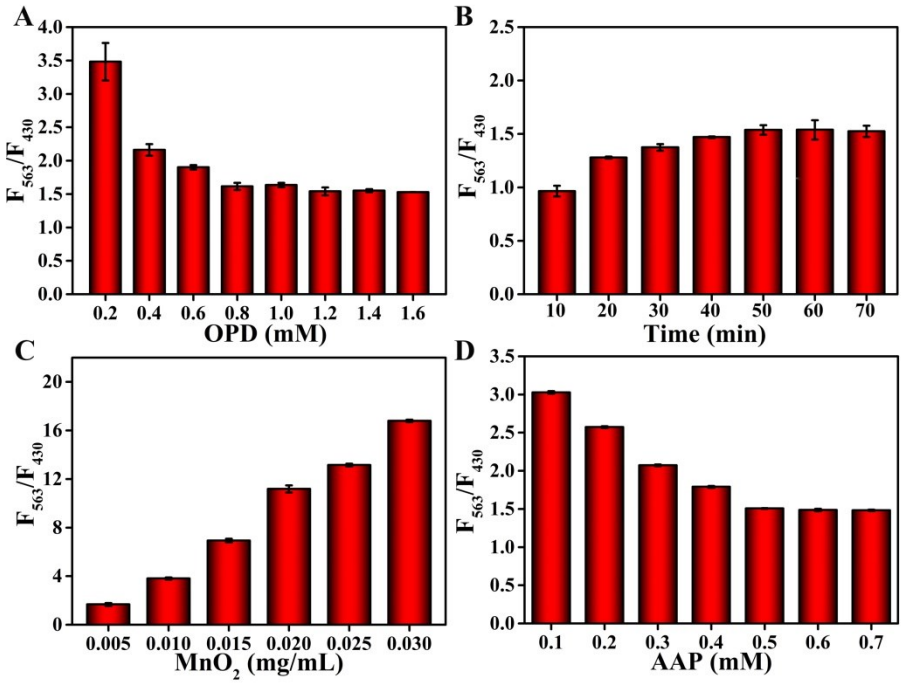

Fig. S10. The F_{563}/F_{430} of the proposed sensing system upon different reaction conditions (A) OPD concentration; (B) incubation time; (C) MnO_2 nanosheets concentration and (D) AAP concentration.

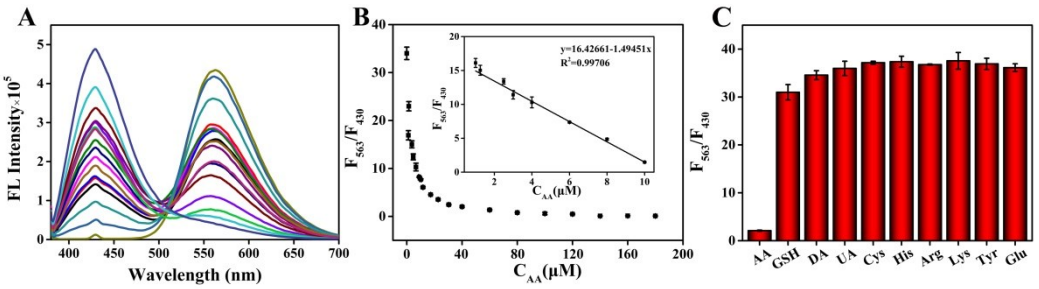

Fig. S11. (A) The fluorescent spectra (λex = 375 nm) of different concentrations of AA; (B) The related linear relationship over the concentration range from 1 to 100 μM AA; (C) The fluorescence intensities ratios of the analytical solution in the presence of other reductive species or amino acids only.

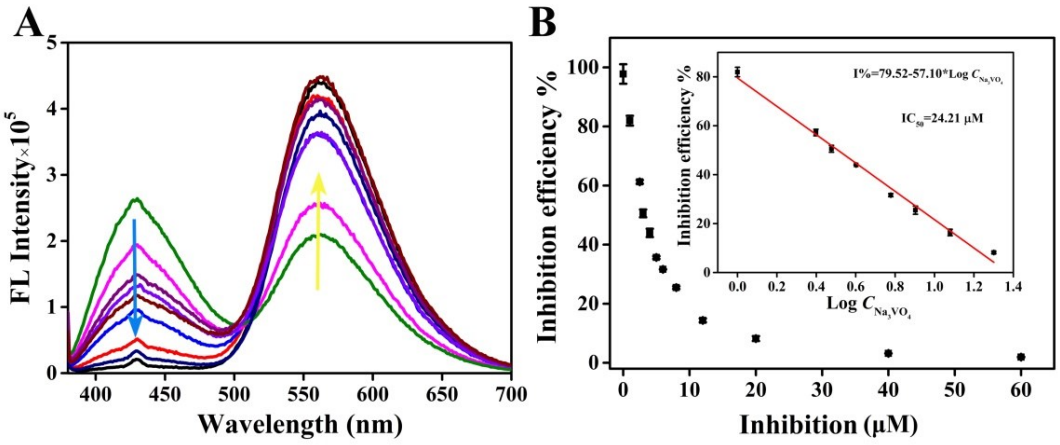

Fig. S12. (A) Fluorescence spectra of the proposed sensing system upon Na_3VO_4 addition with different concentrations in the presence of 10 mU/mL ALP. (B) Relationship plots between the inhibition efficiency of the proposed sensing system and Na_3VO_4 concentration.

Table S1 Comparison of the different methods for ALP detection.

Method	Sensing system	Liner range (mU/mL)	LOD (mU/mL)	Ref.
Fluorometry	g-C_3N_4/CoOOH	1-30	0.92	1
Colorimetry	Fe(II)-phenanthrole	0-220	0.94	2
Colorimetry	Cu^{2+}-HRP–TMB	0-120	5.4	3
Colorimerty	AuNPs-cystine	0.2-20	0.2	4
Fluorometry	Cu(II)-dependent DNAzyme	0.36-54.55	0.14	5
Fluorometry	GQDs-BQ	1-90	0.45	6
Fluorometry	β-CD-CQDs	3.1-80	0.9	7
Fluorometry	$Eu(DPA)_3$@Lap-Cu^{2+}	0.5-60	0.5	8
Fluorometry	CuNCs/Al^{3+}/PPi	0.5-25	0.15	9
Fluorometry	Ag_2S/Calcein	2-100	1.28	10
Fluorometry	Calcein-Ce^{3+}	0.1-0.4,0.4-1.2	0.23	11
Fluorometry	MoS_2 QDs	0.5-5	0.1	12
Fluorometry	SPNs@MnO_2-ALP	0.1-9	0.034	13
Fluorometry	ALP-PDA QDs	0.04–80	0.015	14
Fluorometry	Coumarin@Tb-GMP	25-200	10	15
Fluorometry	ALP-MnO_2-OPD	0.25-10	0.06	This work

Table S2. ALP determination in human serum samples based on the standard addition method.

Samples	Added (mU/mL)	Detected (mU/mL)	Recovery (%)	RSD (%)
	0	2.10	0	0
1	1	3.15	105	2.25
	4	6.10	100	1.80
	0	1.98	0	0
2	1	2.96	98	3.40
	4	6.0	100	1.20

References

(1) Liu, S. G.; Han, L.; Li, N.; Fan, Y. Z.; Yang, Y. Z.; Li, N. B.; Luo, H. Q. A Ratiometric Fluorescent Strategy for Alkaline Phosphatase Activity Assay Based on g-C3N4/CoOOH Nanohybrid via Target-Triggered Competitive Redox Reaction. *Sensor. Actuat B-Chem.* **2019**, *283*, 515-523.

(2) Hu, Q.; Zhou, B.; Dang, P.; Li, L.; Kong, J.; Zhang, X. Facile Colorimetric Assay of Alkaline Phosphatase Activity Using Fe(II)-phenanthroline Reporter. *Anal. Chim. Acta* **2017,** 950,170-177.

(3) Shi, D.; Sun, Y.; Lin, L.; Shi, C.;Wang, G.; Zhang, X. Naked-eye Sensitive Detection ofAlkaline Phosphatase (ALP) and Pyrophosphate (PPi) Based on A Horseradish Peroxidase Catalytic Colorimetric System with Cu(II). *Analyst* **2016,** 141, 5549-5554.

(4) Xianyu, Y. L.; Wang, Z.; Jiang, X. Y. A Plasmonic Nanosensor for Immunoassay via Enzyme Triggered Click Chemistry. *ACS Nano* **2014**, 8, 12741-12747.

(5) Zhao, M. M.; Guo, Y. J.; Wang, L. X.; Luo, F.; Lin, C. Y.; Lin, Z. Y.; Chen, G. N. A Sensitive Fluorescence Biosensor for Alkaline Phosphatase Activity Based on the Cu(II)-dependent DNAzyme. *Anal. Chim. Acta* **2016**, 948, 98-103.

(6) Huang, H.; Wang, B.; Chen, M.; Liu, M.; Leng, Y.; Liu, X.; Li, Y. X.; Liu, Z. N. Fluorescence Turn-on Sensing of Ascorbic Acid and Alkaline Phosphatase Activity Based on Graphene Quantum Dots. *Sensor. Actuat B-Chem.* **2016**, 235, 356-361.

(7) Tang, C., Qian, Z. S., Huang, Y. Y.; Xu, J. M.; Ao, H.; Zhao, M. Z.; Zhou, J.; Chen, J.; Chen, J.R.; Feng, H. A Fluorometric Assay for Alkaline Phosphatase Activity Based on β-cyclodextrin-modified Carbon Quantum Dots through Host-guest Recognition. *Biosens. Bioelectron.* **2016**, 83, 274-280.

(8) Zhao, J. H.; Wang. S.; Lu, S. S.; Sun, J.; Yang, X. R. A Luminescent Europium-dipicolinic Acid Nanohybrid for the Rapid and Selective Sensing of Pyrophosphate and Alkaline Phosphata seactivity. *Nanoscale* **2018,** 10, 7163-7170.

(9) Geng, F.; Zou, C.; Liu, J.; Zhang, Q.; Guo, X.; Fan, Y.; Yu, H.; Yang, S.; Liu, Z.; Li, L.Development of Luminescent Nanoswitch for Sensing of Alkaline Phosphatase in Human Serum Based on Al3+-PPi Interaction and Cu NCs with AIE Properties. *Anal. Chim. Acta* **2019,** 1076,131-137.

(10) Cai, M.; Ding, C.; Wang, F.; Ye, M.; Zhang, C.; Xian, Y. A Ratiometric Fluorescent Assay for the Dtection and Bioimaging of Alkaline Phosphatase Based on Near Infrared Ag_2S Quantum Dots and Calcein. *Biosen. Bioelectron.* **2019**, 137, 148-153.

(11) Chen, C. X.; Zhao J. H., Lu, Y. Z., Sun, J., Yang, X. R. Fluorescence Immunoassay Based on the Phosphate-Triggered Fluorescence Turn-on Detection of Alkaline Phosphatase. *Anal. Chem.,* **2018**, *90*, 3505-3511.

(12) Zhong, Y.; Xue, F.; Wei, P.; Li, R.; Cao, C.; Yi, T. Water-Soluble MoS2 Quantum Dots for Facile and Sensitive Fluorescence Sensing of Alkaline Phosphatase Activity in Serum and Live Cells Based on the Inner Filter Effect. *Nanoscale* **2018**, *10*, 21298-21306.

(13)J. He, X. Jiang, P. Ling, J. Sun and F. Gao, *ACS Omega*, **2019**, 4, 8282-8289.

(14) Q. Yang, X. Wang, H. Peng, M. Arabi, J. Li, H. Xiong, J. Choo and L. Chen, *Sensor. Actuat B-Chem,* **2020**, 302.127176

(15) J. Deng, P. Yu, Y. Wang and L. Mao, *Anal Chem*, **2015**, 87, 3080-3086.